

# Carborane confined nanoparticles for boron neutron capture therapy: Improved stability, blood circulation time and tumor accumulation

著者別名	角谷 省吾, 大石 基, 長崎 幸夫
journal or publication title	Reactive & functional polymers
volume	71
number	7
page range	684-693
year	2011-07
権利	(C) 2011 Elsevier Ltd. NOTICE: this is the author's version of a work that was accepted for publication in Reactive & functional polymers. Changes resulting from the publishing process, such as peer review, editing, corrections, structural formatting, and other quality control mechanisms may not be reflected in this document. Changes may have been made to this work since it was submitted for publication. A definitive version was subsequently published in PUBLICATION, 71, 7, 2011, DOI:10.1016/j.reactfunctpolym.2011.03.010
URL	<a href="http://hdl.handle.net/2241/113545">http://hdl.handle.net/2241/113545</a>

doi: 10.1016/j.reactfunctpolym.2011.03.010

# Carborane Confined Nanoparticles for Boron Neutron Capture Therapy: Improved Stability, Blood Circulation Time and Tumor Accumulation

*Shogo Sumitani<sup>1</sup>, Motoi Oishi<sup>1-3</sup>, Yukio Nagasaki<sup>\*1-5</sup>*

*<sup>1</sup>Institute of Materials Science, Graduate School of Pure and Applied Sciences,  
University of Tsukuba,*

*<sup>2</sup>Tsukuba Research Center for Interdisciplinary Materials Science (TIMS),*

*<sup>3</sup>Center for Tsukuba Advanced Research Alliance (TARA),*

*<sup>4</sup>Master's School of Medical Sciences, Graduate School of Comprehensive Human Sciences,  
University of Tsukuba,*

*<sup>5</sup>Satellite Laboratory, International Center for Materials Nanoarchitectonics (MANA),  
National Institute of Materials Science (NIMS), Tennoudai 1-1-1,  
Tsukuba, Ibaraki 305-8573, Japan*

**Key words:** BNCT, biodegradable polymers, drug delivery systems, core cross-linked micelles.

**Abstract**

Carborane confined nanoparticles based on the core cross-linked and boron-containing micelles (CL micelles) were prepared using the radical polymerization of poly(ethylene glycol)-*block*-poly(lactide) copolymer (PEG-*b*-PLA), which contained an acetal group at the PEG end and a methacryloyl group at the PLA end (acetal-PEG-*b*-PLA-MA), with polymerizable carborane (VB-carborane) as a cross-linker. No leakage of VB-carborane from the CL micelles was observed in PBS even in the presence of 10 % fetal bovine serum (FBS) at 37 °C, whereas significant leakage (80 %) of VB-carborane was observed for the non-cross-linked (NCL) micelles under the same conditions. To clarify the biodistribution of both types of micelles, <sup>125</sup>I (RI: radioisotope)-labeled CL and NCL micelles were injected into tumor-bearing BALB/c mice via the tail vein. The <sup>125</sup>I-labeled CL micelles showed a remarkably prolonged blood circulation time (7.9 %ID/g) and high tumor accumulation (2.9 %ID/g) compared with the <sup>125</sup>I-labeled NCL micelles (blood: 3.1 %ID/g, tumor: 1.8 %ID/g) at 24 h after injection. Moreover, the biodistribution of the VB-carborane (boron species) was also evaluated using ICP-MS at 24 h after intravenous injection of the CL and NCL micelles. The boron concentrations in blood and tumor after injection of the CL micelles (blood: 13.5 %ID/g, tumor: 5.4 %ID/g) were also significantly higher than the concentrations after the injection of the NCL micelles (blood: 1.8 %ID/g, tumor: 1.4 %ID/g). Note that the biodistribution of the boron species in the CL micelles was similar to that of the <sup>125</sup>I-labeled CL micelles, whereas the boron concentrations (%ID/g) in blood and tumor after injection of the NCL micelles were lower than those expected with the <sup>125</sup>I concentrations (%ID/g) in blood and tumor. Thus, the boron concentration ratios of the CL micelles to the NCL micelles ( $CL_{ICP}/NCL_{ICP}$ ) in blood (15.8) and tumor (3.8) were much higher than the <sup>125</sup>I concentration ratios of  $CL_{RI}/NCL_{RI}$  in blood (2.5) and tumor (1.6). These differences might be caused by the suppression of the leakage of the VB-carborane from the CL micelles in the blood stream due to the existence of the cross-linking bonds between the VB-carborane and the PLA core.

Based on these results, the CL micelles composed of PEG-*b*-PLA copolymer cross-linked by carborane represent a promising approach to the creation of a novel boron carrier for boron neutron capture therapy (BNCT).

## 1. Introduction

Boron neutron capture therapy (BNCT) has attracted much attention as a selective and noninvasive cancer therapy using boron-10 ( $^{10}\text{B}$ ) compounds, which efficiently generate cytotoxic  $\alpha$ -particles and  $^7\text{Li}$  nuclei within the cell diameter (5-9  $\mu\text{m}$ ) through the nuclear reaction of the  $^{10}\text{B}$  atom with low-energy thermal neutrons.<sup>[1],[2]</sup> Two types of the  $^{10}\text{B}$ -compounds, sodium borocaptate (BSH) and L-4-dihydroxyboronylphenylalanine (BPA), have been approved for clinical trials so far. Due to the rapid clearance of these compounds from the blood stream (blood circulation time of BSH:  $t_{1/2} < 1 \text{ h}$ )<sup>[3]</sup> a high dose of the  $^{10}\text{B}$ -compound is generally required to allow a sufficient concentration of the  $^{10}\text{B}$ -compound to accumulate in the tumor tissue (20-30  $\mu\text{g}$  of  $^{10}\text{B}$  atoms per gram of tumor tissue). Additionally, the non-specific distribution of these compounds also reduces the efficiency of their accumulation in the tumor tissue. To improve the effect of BNCT, the effective accumulation of boron compounds in the area of the tumor tissue is one of the key issues.

A promising strategy in this regard is the concept of drug delivery systems (DDS). Matsumura and Maeda et al. have reported that a DDS based on nanomaterials, including proteins, drug-conjugated polymers and nano-sized particles, enabled the accumulation of drug in the tumor tissue due to the so-called “enhanced permeability and retention” (EPR) effect.<sup>[4],[5]</sup> Indeed, PEG-modified liposomes have been reported to be effective nano-sized carriers of hydrophilic and negatively charged BSH, thus enhancing biocompatibility, blood circulation time and accumulation in the tumor tissue. Although the PEG-modified liposomes

encapsulating the BSH showed higher accumulation in the tumor tissues compared to the free BSH due to the EPR effect,<sup>[6]-[8]</sup> the therapeutic efficacy of the PEG-modified liposomes encapsulating the BSH is still controversial due to the leakage of the encapsulated BSH from the liposome into the blood stream caused by the high ion osmotic pressure of the BSH-loaded interior of the liposome.<sup>[9]</sup> An alternative approach is the <sup>10</sup>B-compound-conjugated liposomes fabricated by covalently linking a lipid (hydrophobic group) with a <sup>10</sup>B-compound (hydrophilic group) to suppress the leakage of the <sup>10</sup>B-compound into the blood stream.<sup>[10]-[12]</sup> The <sup>10</sup>B-compound-conjugated liposome constructed from *nido*-carborane afforded a sufficiently high <sup>10</sup>B concentration in the tumor tissue, without leakage of the <sup>10</sup>B compound into the blood stream. However, the synthesis of *nido*-carborane required complicated preparation steps. Additionally, serious acute toxicity was observed *in vivo* because of the cytotoxicity of *nido*-carborane.<sup>[11]</sup> Thus, the development of a <sup>10</sup>B-compound confined delivery system, which does not allow leakage of the <sup>10</sup>B-compound and is not toxic is a promising approach to cancer BNCT.

Recently, a new class of drug delivery system has emerged, based on nano-sized polymeric micelles composed of PEG-*block*-poly(D,L-lactide) (PLA) copolymers (PEG-*b*-PLA) because the PEG-*b*-PLA micelles showed high biocompatibility, nontoxicity, long blood circulation time and high biodegradability.<sup>[13]-[16]</sup> The hydrophobic PLA core is able to accommodate hydrophobic drugs, and the brush-like hydrophilic PEG shell prevents protein adsorption and subsequent non-specific uptake by the reticuloendothelial system (RES) after intravenous injection. However, Chen et al. reported that hydrophobic fluorescent compounds incorporated into the core of the PEG-*b*-PLA micelle showed a loss of micelle integrity within the blood stream due to the interaction between the micelles and some blood components, leading to the rapid leakage of the hydrophobic fluorescent compounds within 15 min after intravenous injection.<sup>[17]</sup> To solve this problem, many studies have focused on the

stabilization of micelles, introducing chemical linkages into either the shell or the core segment to avoid the loss of micelle integrity.<sup>[18]-[20]</sup> We have also previously reported the preparation of core-polymerized PEG-*b*-PLA micelles possessing a methacryloyl group at the PLA chain end. Through the radical polymerization,<sup>[21],[22]</sup> the core-polymerized micelles eventually showed high dispersibility even after lyophilization as well as high stability against dilution, temperature changes and sodium dodecyl sulfate solution. Indeed, these above-mentioned approaches (polymerized or cross-linked micelles) are critical to the formulation of micelles that are resistant to the loss of micelle integrity. However, even though the polymerized or cross-linked micelles are employed, the leakage of the drug from the polymerized or cross-linked micelles is not completely suppressed due to the diffusion of the drug from the core to the blood stream when the drug is physically entrapped inside the core by hydrophobic interactions.<sup>[23],[24]</sup>

In this study, we designed and prepared a core cross-linked and boron-containing micelles (CL micelles) using the radical copolymerization of PEG-*b*-PLA, which contains an acetal group at the PEG end and a methacryloyl group at the PLA end (acetal-PEG-*b*-PLA-MA), with hydrophobic 1,2-bis(4-vinylbenzyl)-*clos*o-carborane (model for <sup>10</sup>B-compound) as a cross-linker (**Fig. 1**). Note that the CL micelles suppress the leakage of carborane and the loss of micelle integrity in the blood stream, leading to a prolonged blood circulation time and enhanced accumulation in tumor tissues. The cross-linked core of the micelle is anticipated to gradually collapse through the biodegradation of the PLA segment after the therapy. Moreover, an acetal group at the tethered PEG chain end can be easily converted to an aldehyde group by hydrolysis with acid. The aldehyde group is known to easily react with hydrazide compounds, facilitating the installation of tumor-specific ligand molecules and radioactive tags for monitoring the biodistribution. We believe that the use of the CL micelles composed of acetal-PEG-*b*-PLA-MA and 1,2-bis(4-vinylbenzyl)-*clos*o-carborane represents a

promising strategy for the fabrication of drug delivery systems, which deploy a sufficient quantity of  $^{10}\text{B}$  to tumor tissues.

## 2. Experimental Section

### 2.1. Materials and methods

Azobisisobutyronitrile (AIBN; Wako Pure Chemical Industries, Ltd., Osaka, Japan) was purified by recrystallization from methanol and dried *in vacuo*. *N,N*-Dimethylacetamide (DMAc; Kanto Chemicals Co., Ltd., Tokyo, Japan), L-tyrosine hydrazide (Tokyo Chemical Industry Co., Ltd., Tokyo, Japan), sodium cyanoborohydride (Aldrich Chemical Co., Ltd., Milwaukee, WI, USA), *p*-toluenesulfonchloramide sodium salt (chloramine T; Kanto Chemicals Co., Ltd.) and sodium peroxodisulfate (Kanto Chemicals Co. Ltd.) were used as received. Water was purified using the Milli-Q system (Millipore). Dynamic light scattering measurements were conducted in phosphate buffered saline (PBS) at 37 °C using a Zetasizer Nano-ZS instrument (Malvern, UK) equipped with a 4.0 mW He–Ne laser (633 nm). Zeta potential measurement of the micelles was performed at 37 °C in 5 mM phosphate buffer solution at pH 7.4 using a Zetasizer Nano ZS.  $^1\text{H}$ -NMR spectra were obtained in chloroform-*d* at 25 °C with a JEOL EX270 spectrometer (JEOL, Japan). Chemical shifts were reported in ppm relative to  $\text{CDCl}_3$  ( $\delta$  7.26 ppm). Fluorescence spectra were recorded on an F-7000 spectrometer (Hitachi, Japan). The concentration of boron atoms was determined with ICP-AES using an ICAP-575 emission spectrometer (Nippon Jarrell-Ash, Japan) and ICP-MS using an ELAN DRC II (PerkinElmer, Inc., USA). 1,2-Bis(4-vinylbenzyl)-*closo*-carborane (VB-carborane) was synthesized according to a previous study,<sup>[25]</sup> and the detailed procedure is described in the supporting information section. Acetal-PEG-*b*-PLA-MA was synthesized

according to our previous study,<sup>[21]</sup> and the molecular weight of the PEG segment and the PLA segment of the block copolymer were estimated to be 9,500 and 5,000 g/mol. The block copolymer with the above-stated molecular weight was reported to form spherical micelles in aqueous solution<sup>[34]</sup> and to be stable in the presence of serum proteins.<sup>[24]</sup> Acetal-PEG-*b*-PLA-MA micelles were also prepared according to our previous study.<sup>[21]</sup> The average diameter and size distribution ( $= \mu_2/\Gamma^2$ ) of the acetal-PEG-*b*-PLA-MA micelles were found to be 45.8 nm and 0.135, respectively, as determined using DLS measurement. The cytotoxicity of NCL micelles, CL micelles, free VB-carborane, BPA and BSH were evaluated using the WST-8 assay, which is described in detail in the supporting information section (see supporting information, Fig. S4).

All animal experiments were conducted humanely after approval from the Institutional Animal Experiment Committee of the University of Tsukuba and complied with the Regulations for Animal Experiments at our university and the Fundamental Guidelines for Proper Conduct of Animal Experiments and Related Activity in Academic Research Institutions under the jurisdiction of the Ministry of Education, Culture, Sports, Science and Technology.

## **2.2. Preparation of the NCL and CL micelles**

A solution of VB-carborane (45 mg) and AIBN (1.5 mg) in chloroform (3.0 mL) was added dropwise to 100 mL of a stirred acetal-PEG-*b*-PLA-MA micelles solution in water (1.0 mg/L) to form oil in water (o/w) emulsion. After the o/w emulsion was maintained for 1 h and the solution was exposed to air at 25 °C for 3 h to evaporate the chloroform, the resulting micelle solution was purged with nitrogen gas for 20 min to completely remove the remaining

chloroform and dissolved oxygen. To prepare the cross-linked micelles (CL micelles), polymerization was conducted at 60 °C for 24 h. Purification was performed using repeated ultrafiltrations using a membrane with a molecular weight cut-off of 100,000 (VIVASPIN 4, Sartorius Stedim Biotech, Germany). For controls, non-cross-linked micelles (NCL micelles) encapsulating VB-carborane were prepared using the same procedure as that for CL micelles, except for the addition of AIBN and heating. To determine the average size and size distribution of the micelles, DLS measurement was performed in PBS at 37 °C. To confirm the encapsulation of VB-carborane into the micelles, the gel filtration chromatography was conducted on a PD-10 column (GE Healthcare, USA) using PBS as the eluent, and the boron atom concentration and light scattering intensity of each collected fraction were measured using ICP-AES and DLS, respectively. The loading content and efficiency of the boron atoms in the micelles were determined using ICP-AES according to a previous paper.<sup>[26]</sup> To determine whether the VB-carborane was covalently cross-linked in the core of the micelles, <sup>1</sup>H-NMR analysis of the lyophilized NCL and CL micelles was conducted in CDCl<sub>3</sub> at 25 °C.

### **2.3. Leakage of VB-carborane from the NCL and CL micelles**

The NCL or CL micelle solution (1.0 mg/mL, 10 mL), with or without 10 % FBS, was poured into dialysis bags (MWCO: 100,000), and each bag was immersed in 90 mL of PBS with or without 10 % FBS at 37 °C. At a definite time interval, 0.5 mL of the solution inside the dialysis bag was sampled, and a fluorescence measurement was performed to determine the amount of VB-carborane that remained in each micelle based on the fluorescence intensity of the VB-carborane ( $\lambda_{\text{ex}}$ : 339 nm,  $\lambda_{\text{em}}$ : 380 nm).

### **2.4. Stability of the micelles against serum protein**

The NCL or CL micelle solution (1.0 mg/mL, 90  $\mu$ L) was added to 10  $\mu$ L of FBS, followed by incubation at 37  $^{\circ}$ C for 24 h. After a ten-fold dilution of the sample solutions and filtration through a 0.45  $\mu$ m filter, 50  $\mu$ L aliquots were subjected to SEC analysis using a JASCO HPLC system (JASCO, Tokyo, Japan) equipped with a refractive index (RI) detector (RI-2031), a fluorescence detector (FP-2020), and a Superose 6 10/30 GL column (GE Healthcare, USA) with 10 mM phosphate buffer (pH 7.4) at a flow rate of 0.50 mL/min at 40  $^{\circ}$ C.

## 2.5. Conjugation of tyrosine residues with NCL and CL micelles

To clarify the biodistribution of the micelles, the preparation of  $^{125}$ I (RI: radioisotope)-labeled NCL and CL micelles were performed. Consistent with previous papers,<sup>[16],[30]</sup> a tyrosine residue (Tyr), as a site of radiolabeling, was introduced onto the NCL or CL micelles. An aqueous solution of NCL or CL micelles bearing acetal groups (10.0 mL, 2.0 mg/mL) was adjusted to pH 2 using 1.0 M hydrochloric acid, and the resulting solution was stirred for 2 h at room temperature to prepare NCL or CL micelles with aldehyde groups. Purification was performed with dialysis against a large quantity of water (2.0 L) using a pre-swollen semi-permeable membrane (MWCO. 12,000–14,000) for 24 h. The dialysate water was exchanged at 2, 5 and 8 h after the beginning of dialysis. After the purification, 3.0 mL of the solution was freeze-dried to determine the concentration and the degree of the functionality of the aldehyde group in the  $^1$ H-NMR spectra. As a typical example, the  $^1$ H-NMR spectra of both the NCL and the CL micelles in  $\text{CDCl}_3$  showed a new signal at 9.8 ppm, which can be attributed to the aldehyde group, along with the disappearance of the acetal signal at 4.8 ppm (see supporting information, **Fig. S5**), indicating that more than 90 %

of the acetal groups of both the NCL and the CL micelles can be converted to aldehyde groups. To a solution of the NCL or CL micelles bearing aldehyde groups (10.0 mL, 1.3 mg/mL, [aldehyde] = ca. 90  $\mu$ M) in 10 mM phosphate buffer (pH = 6.5), L-tyrosine (Tyr) hydrazide (10.8 mg, 55  $\mu$ mol) was added, and the reaction mixture was stirred at room temperature for 1 h. Next, sodium cyanoborohydride (3.5 mg, 51  $\mu$ mol) was added as a reducing agent to reduce the unstable hydrazone linkage (C=N-NH-), and then the mixture was stirred at room temperature for 24 h. Purification was performed with dialysis against a large quantity of water (2.0 L) using a pre-swollen semi-permeable membrane (MWCO: 12,000–14,000) for 3 days. The dialysate water was exchanged at 2, 5, 8, 24 and 48 h after the beginning of dialysis. After purification, 3.0 mL of the solution was freeze-dried to determine the concentration and the degree of the functionality of the Tyr residue in the  $^1\text{H-NMR}$  spectra. The  $^1\text{H-NMR}$  spectra of the lyophilized NCL or CL micelles in DMSO-*d* at 80 °C showed the aromatic protons of the Tyr residue, and the degree of functionality of the Tyr residue of the NCL and CL micelles was 45 % and 38 %, respectively, as determined from the peak intensity ratio of the aromatic protons in Tyr ( $\delta$  6.8 and 7.2 ppm) to the methine proton in the PLA segment ( $\delta$  5.2 ppm) of the block copolymer (see supporting information, Fig. S6).

## 2.6. Radiolabeling of the Tyr-NCL and Tyr-CL micelles

A solution of Na $^{125}\text{I}$  in 10 mM phosphate-buffered saline (PBS) (15  $\mu$ L, 74 MBq/mL, PerkinElmer, Inc., USA) was added to a solution of Tyr-NCL or Tyr-CL micelles in 10 mM PBS (300  $\mu$ L, 2.0 mg/mL). A solution of chloramine T in 10 mM PBS (100  $\mu$ L, 2.0 mM) was added to the reaction mixture, which was incubated at room temperature for 10 min. Next, the reaction was quenched by the addition of a solution of sodium peroxodisulfate in 10 mM PBS

(100  $\mu$ L, 40 mM). After shaking for a few minutes, the unreacted  $^{125}\text{I}$  and other chemicals were removed by passing the sample through a PD-10 column (GE Healthcare, USA) using PBS as an eluent prior to the biodistribution study. The radioactivity of each fraction was measured using a  $\gamma$ -counter (Aloka, Japan) (see supporting information, Fig. S7).

## **2.7. Biodistribution of the $^{125}\text{I}$ -labeled Tyr-NCL and $^{125}\text{I}$ -labeled Tyr-CL micelles**

The biodistribution of the  $^{125}\text{I}$ -labeled Tyr-NCL and  $^{125}\text{I}$ -labeled Tyr-CL micelles was evaluated in tumor-bearing, 5-week-old-male BALB/c mice ( $n = 4$ , Charles River, Japan). Each tumor-bearing mouse was prepared with a subcutaneous injection of colon-26 cells ( $1.0 \times 10^6$  cells/mouse) into its back. When the volume of the tumor reached  $100 \text{ mm}^3$ , the  $^{125}\text{I}$ -labeled Tyr-NCL micelles or  $^{125}\text{I}$ -labeled Tyr-CL micelles were administered to the tumor-bearing mice by intravenous injection at a dose of 1.3 mg micelles per kg body weight. The blood, liver, spleen, kidney and tumor samples were collected, using sodium pentobarbital (40 mg/kg) as an anesthetic, at defined time periods after the micelle injection. The radioactivity and the weight of the collected samples were measured using a  $\gamma$ -counter and a balance, respectively. The total volume of blood in each mouse was estimated using the following equation<sup>[32]</sup>:

$$\text{Total blood volume (mL)} = \text{body weight (g)} \times 8.45/100 \text{ (mL/g)}$$

## **2.8. Biodistribution of the boron species in the NCL and CL micelles**

The biodistribution of the boron species of the NCL and CL micelles in tumor-bearing mice was evaluated using ICP-MS. The tumor-bearing mice were prepared with a subcutaneous injection of colon-26 cells ( $1.0 \times 10^6$  cells/mouse) into its back. When the volume of the

tumor reached 100 mm<sup>3</sup>, the NCL or CL micelles were administered to the tumor-bearing mice by intravenous injection at a dose of 0.20 mg boron atoms per kg body weight. The blood, liver, spleen, kidney and tumor samples were collected, using sodium pentobarbital (40 mg/kg) as an anesthetic, at 24 h after the injection. The excised tissues were weighed and digested with 2 mL of HNO<sub>3</sub> (ultratrace analysis grade, Wako, Japan) at 90 °C for 3 h, and then the dissolved samples were diluted with distilled water. After filtering through a 0.45 μm filter, the boron concentration was measured using ICP-MS.

### 3. Results and Discussion

#### 3.1. Preparation and characterization of the NCL and CL micelles

Consistent with previous literature,<sup>[21]</sup> acetal-PEG-*b*-PLA-MA was synthesized by the successive anionic ring-opening polymerization of EO using potassium 3,3-diethoxy-1-propanolate as an initiator, followed by the addition of D,L-lactide. The resulting block copolymer with a reactive potassium alkoxide terminus was capped by adding an excess of methacrylic anhydride to introduce a polymerizable methacryloyl group at the PLA chain end (supporting information, Scheme S1). The molecular weights of the PEG and PLA segments in the acetal-PEG-*b*-PLA-MA were found to be 9,500 and 5,000, respectively, as determined with SEC and <sup>1</sup>H-NMR analysis (supporting information, **Fig. S1** and **S2**). These are in good agreement with the theoretical values (PEG;  $M_n = 9,500$ , PLA;  $M_n = 5,000$ ) obtained based on the initial monomer/initiator ratio. The SEC analysis also revealed that the acetal-PEG-*b*-PLA-MA had a narrow molecular weight distribution ( $M_w/M_n = 1.12$ ). The degree of functionality of the acetal and the methacryloyl groups was found to be 95 and 99 %, respectively, as determined with <sup>1</sup>H-NMR analysis. The VB-carborane was synthesized

according to the previous literature;<sup>[25]</sup> viz., lithiation of both methine protons (CH) of *o*-carborane was performed using 2.0 equiv. of BuLi in THF, followed by the addition of 2.0 equiv. of 4-vinylbenzyl chloride (supporting information, Scheme S2). The VB-carborane was obtained in 21 % yield after purification with column chromatography. The VB-carborane showed fluorescence in methanol ( $\lambda_{\text{ex}}$ : 339 nm,  $\lambda_{\text{em}}$ : 380 nm), indicating that VB-carborane can be used not only as a model compound for <sup>10</sup>B-compounds but also as a fluorescent probe.

To prepare the acetal-PEG-*b*-PLA-MA micelles, the dialysis method was employed in this study because this method is known to form micelles with a relatively narrow size distribution. Block copolymer was first dissolved in DMAc, which is a good solvent for both the PEG and the PLA segment and the solution was dialyzed against water for 24 h. The average diameter of the acetal-PEG-*b*-PLA-MA micelles was 45.8 nm with a narrow size distribution ( $\mu_2/\Gamma^2 = 0.135$ ), as determined with DLS measurement. Encapsulation of VB-carborane in the acetal-PEG-*b*-PLA-MA micelles was performed with the conventional solvent evaporation method using chloroform. This is a typical method for encapsulating hydrophobic drugs into the hydrophobic core of polymeric micelles through the hydrophobic interactions.<sup>[27],[28]</sup> The average diameter of the VB-carborane-encapsulating acetal-PEG-*b*-PLA-MA micelles (NCL micelles) increased from 45.3 nm to 81.1 nm as shown in **Fig. 2**. This is probably due to the formation of a loosely associated PLA core as a result of the swelling of the hydrophobic PLA core upon the addition of chloroform.<sup>[24]</sup> To prepare the CL micelles, both VB-carborane and AIBN were encapsulated into acetal-PEG-*b*-PLA-MA micelles using the solvent evaporation method, and the polymerization of the core was conducted at 60 °C for 24 h. The characteristics of the NCL and CL micelles are summarized in **Table 1**. The average diameter and size distribution (85.3 nm,  $\mu_2/\Gamma^2 = 0.171$ ) of the CL micelles were almost similar to those

of the NCL micelles (81.1 nm,  $\mu_2/\Gamma^2 = 0.158$ ), suggesting that the core polymerization process does not influence the average diameter or size distribution of the micelles.

To confirm the encapsulation of VB-carborane into the CL micelles, column fractionation by gel filtration chromatography was conducted using PBS as the eluent, and the boron atom concentration and light scattering intensity of each collected fraction were measured using ICP-AES and DLS, respectively (**Fig. 3**). The boron atoms were detected in the 3 and 4 mL fractions, and a significant increase in the light scattering intensity was also observed in the same fractions due to the co-existence of boron atoms and micelles in the solution. These findings indicate that VB-carborane was obviously encapsulated into the CL micelles. The loading content of boron atoms in the NCL and CL micelles was determined to be 0.29 wt% (loading efficiency: 3.2 %) and 0.26 wt% (loading efficiency: 3.1 %), respectively, as summarized in **Table 1**. The loading content of boron atoms in the CL micelles was similar to that in the NCL micelles, strongly indicating that leakage of VB-carborane from the micelles did not occur at all during the polymerization process.

To clarify whether the VB-carborane was covalently cross-linked in the core of the micelles,  $^1\text{H-NMR}$  analysis of the lyophilized NCL and CL micelles was conducted in  $\text{CDCl}_3$ , which is a good solvent for both acetal-PEG-*b*-PLA-MA and VB-carborane (**Fig. 4**). In the case of the NCL micelles, the protons attributed to the methacryloyl end group were clearly observed at 5.6 and 6.2 ppm, and vinyl protons of VB-carborane were observed at 5.7 and 6.7 ppm. These findings indicate that both acetal-PEG-*b*-PLA-MA and VB-carborane were obviously dissolved in  $\text{CDCl}_3$ . However, both the methacryloyl and the vinyl protons disappeared in the  $^1\text{H-NMR}$  spectrum of the CL micelles, suggesting that the copolymerization (cross-linking) of the acetal-PEG-*b*-PLA-MA and VB-carborane proceeded with high conversion into the core of the micelles.

### 3.2. Leakage of VB-carborane from the NCL and CL micelles

The leakage of the encapsulated  $^{10}\text{B}$ -compound from nano-sized carriers under physiological conditions in the presence of serum proteins is an important issue for *in vivo* application. The leakage of VB-carborane from the NCL and CL micelles was evaluated at 0.2 mg of micelles per mL, well above the critical association concentration (ca. 2.0  $\mu\text{g/mL}$ ), under physiological conditions in the presence or absence of 10 % FBS, because the dissociation of the micelles occurs below the critical association concentration. The amount of VB-carborane remaining in the micelles was determined based on the fluorescence intensity of VB-carborane ( $\lambda_{\text{ex}}$ : 339 nm,  $\lambda_{\text{em}}$ : 380 nm). **Fig. 5** shows the time courses of the leakage of VB-carborane from the NCL and the CL micelles. Almost no leakage of VB-carborane was observed from either the NCL or the CL micelles in the absence of FBS (**Fig. 5(a)**), due to the sufficiently strong hydrophobic interaction between VB-carborane and the hydrophobic PLA core of the NCL micelles. In sharp contrast, significant amounts of VB-carborane were immediately leaked from the NCL micelles in the presence of FBS, and eventually only 20 % of the VB-carborane was still encapsulated in the NCL micelles after 48 h (**Fig. 5(b)**). There are several reports on the leakage of hydrophobic drugs from polymeric micelles in the presence of protein, due to the loss of micelle integrity caused by the interaction between some blood components ( $\alpha$ - and  $\beta$ -globulin and/or BSA) and the micelles.<sup>[17],[29],[31]</sup> Notably, the CL micelles showed no leakage of VB-carborane even in the presence of FBS. The significantly reduced leakage of VB-carborane from the CL micelles results from the highly stable core-shell structure of these micelles and the absence of VB-carborane diffusion from the core to the solution is due to the existence of the cross-linking bonds between the VB-carborane and the PLA core.

### 3.3. Stability of the micelles against serum proteins

To obtain further information on the stability of the NCL and CL micelles in the presence of serum proteins, SEC analyses of the NCL or CL micelles were performed at 0 h (micelle alone) and 24 h after co-incubation with 10 % FBS at 37 °C. The SEC analyses were monitored by fluorescence ( $\lambda_{\text{ex}}$  339 nm,  $\lambda_{\text{em}}$  380 nm) and RI detection. As shown in **Fig. 6(a)** and **6(b)**, the peaks attributed to the NCL and CL micelles were observed by both fluorescence and RI detection at 14 min in the region of the exclusion limit ( $M_n > 300,000$ ) because the VB-carborane was encapsulated in the micelles. Additionally, the small peak at 33 min ( $M_n = \text{ca. } 13,000$ ) was observed only by the RI detection, due to the existence of a small amount ( $< 3\%$ ) of free polymer.<sup>[21]</sup> **Fig. 6(c)** and **6(d)** show the SEC chromatograms of the NCL and CL micelles at 24 h after co-incubation with 10 % FBS. In the case of the NCL micelles, two peaks were detected by both fluorescence and RI detection; viz., the peaks at 14 and 27.5 min correspond to the micelles and the serum albumin, respectively (**Fig. 6(c)**). This clearly indicates that the leakage of VB-carborane from the NCL micelles occurred, presumably due to the loss of micelle integrity and/or diffusion of VB-carborane from the core to the solution. Consequently, the leaked VB-carborane interacted with serum albumin to form a VB-carborane/albumin complex, which was detected at 27.5 min with the fluorescence detection. Note that a 47 % decrease in the area of the NCL micelle peak at 14 min was observed, along with a 48 % increase in the area of the free polymer peak at 33 min with RI detection, suggesting a loss of micelle integrity caused by the interaction between the NCL micelles and serum albumin. On the contrary, the CL micelles showed no fluorescence peak at 27.5 min, attributable to serum albumin at 24 h, even after co-incubation with 10 % FBS (**Fig. 6(d)**); viz., no leakage of the VB-carborane from the CL micelles had occurred. It

should also be noted that almost no change in the area of either the CL micelle peak at 14 min or the free polymer peak at 33 min was observed with the RI detection, indicating that no loss of micelle integrity and no diffusion of VB-carborane from the core to the solution occurred, due to the existence of the covalent bonds between VB-carborane and the PLA core of the micelles. Thus, the CL micelles showed minimal interaction with the serum components due to its highly stable core-shell structure made possible by cross-linking bonds between the VB-carborane and the PLA core, which reduced the leakage of VB-carborane and prevented the loss of micelle integrity even in the presence of 10 % FBS.

### 3.4. Biodistribution of the $^{125}\text{I}$ -labeled of Tyr-NCL and $^{125}\text{I}$ -labeled Tyr-CL micelles

The cytotoxicity of the CL micelles is one of the important issues for the development of BNCT *in vivo*. The cytotoxicity of the NCL micelles, CL micelles, VB-carborane, BPA and BSH against colon-26 cells was evaluated in the presence of 10% FBS in the cell culture medium as shown in Figure S4. Note that the CL micelles and BSH showed no toxicity even at high concentration ( $[\text{B}] = 6.0 \text{ mM}$ ). In contrast, 50 % inhibitory concentration ( $\text{IC}_{50}$ ) values of the NCL micelles, VB-carborane, and BPA were 4.2 mM, 2.6 mM, and 4.7 mM, respectively. Although the cytotoxicity of the VB-carborane ( $\text{IC}_{50} = 2.6 \text{ mM}$ ) is slightly higher than that of the BPA ( $\text{IC}_{50} = 4.7 \text{ mM}$ ), the cytotoxicity of the NCL micelles ( $\text{IC}_{50} = 4.2 \text{ mM}$ ) was similar to that of the clinically approved BPA ( $\text{IC}_{50} = 4.7 \text{ mM}$ ). Moreover, the cytotoxicity of the VB-carborane is lower than that of the *nido*-carborane derivative ( $\text{IC}_{50} = 0.5 \text{ mM}$ ),<sup>[33]</sup> which has been used in the  $^{10}\text{B}$ -compound-conjugated liposomes<sup>[10]-[12]</sup>. These results indicate that the cytotoxicity of VB-carborane was negligible in BNCT. Notably, the cytotoxicity of the CL micelles ( $\text{IC}_{50} = \text{not determined}$ ) was significantly lower than that of the NCL micelles ( $\text{IC}_{50} = 4.2 \text{ mM}$ ). These results indicate that the leakage of the

VB-carborane from the NCL micelles occurred in the presence of 10% FBS, leading to the cytotoxicity caused by the free VB-carborane. In sharp contrast, the leakage of VB-carborane from the CL micelles was suppressed even in the presence of 10% FBS because the VB-carborane was conjugated with the core of micelles through the covalent bonds. It can be concluded that the CL micelle system formulated by the polymerization of acetal-PEG-*b*-PLA-MA and newly synthesized VB-carborane is utilized for BNCT from the standpoint of the cytotoxicity.

To clarify the effect of cross-linkage on the biodistribution of the micelles, the preparation of <sup>125</sup>I (RI: radioisotope)-labeled NCL and CL micelles were performed by employing the acetal group at the PEG end. Thus, the acetal groups at the PEG end of the NCL and CL micelles were hydrolyzed using acid to obtain the reactive aldehyde groups (supporting information, **Fig. S5**), followed by the addition of L-tyrosine hydrazide (Tyr) and sodium cyanoborohydride as a reducing agent. In the <sup>1</sup>H-NMR spectra of the NCL and CL micelles, the degree of Tyr functionality in the NCL and CL micelles was determined to be 45 and 38 %, respectively, based on the integral ratio of the peaks between the aromatic protons of the tyrosine residues (6.98 and 7.30 ppm) and methine protons of the PLA segments (5.51 ppm) (supporting information, **Fig. S6**). The characteristics of the Tyr-conjugated NCL (Tyr-NCL) and CL (Tyr-CL) micelles are also summarized in **Table 1**. Although the Tyr-NCL and Tyr-CL micelles bear the primary amino group and the hydrazone linkage around the PEG end (supporting information, **Fig. S6**), their average diameter and zeta potential were almost consistent with those of the NCL and CL micelles before the installation of the Tyr group. Thus, the effect of the Tyr groups on the biodistribution of the NCL and CL micelles is not considered. <sup>125</sup>I-labeling was conducted using the conventional chloramine T method, followed by purification with gel chromatography (supporting information, **Fig. S7**). The radioactivity levels of the <sup>125</sup>I-labeled Tyr-NCL and Tyr-CL

micelles in the blood, liver, spleen, kidney and tumor samples are expressed as a percentage of the injected dose per gram of tissue (%ID/g) at specified times after intravenous administration in tumor-bearing mice, as shown in **Fig. 7**. There were no differences in the distribution in the liver and spleen between the  $^{125}\text{I}$ -labeled Tyr-NCL and the Tyr-CL micelles (**Fig. 7(b), 7(d)**). In sharp contrast, the concentration of  $^{125}\text{I}$ -labeled Tyr-NCL micelles in the blood was approximately 30 %ID/g, even 10 min after administration, whereas almost all the  $^{125}\text{I}$ -labeled Tyr-CL micelles (43 %ID/g) remained in the blood stream at the same time (**Fig.7(a)**). This suggests that a portion of the  $^{125}\text{I}$ -labeled Tyr-NCL micelles were immediately eliminated from the blood stream after injection because the  $^{125}\text{I}$ -labeled Tyr-NCL micelles showed a higher radioactivity level compared to the  $^{125}\text{I}$ -labeled Tyr-CL micelles in the kidney after 10 min (**Fig.7(c)**). Note that 7.8 %ID/g of  $^{125}\text{I}$ -labeled Tyr-CL micelles still remained in the blood stream after 24 h, whereas only 3.1 %ID/g of  $^{125}\text{I}$ -labeled Tyr-NCL micelles remained after 24 h (**Fig. 7(a)**). These results indicate that the Tyr-CL micelles were poorly eliminated from the blood stream through renal clearance due to the enhancement of the stability of the micelles against serum proteins and/or dilution in the blood stream caused by the introduction of cross-linking bonds between the VB-carborane and the PLA core. It should be noted that the  $^{125}\text{I}$ -labeled Tyr-CL micelles accumulated in higher amounts in the tumor tissue (2.9 %ID/g) compared with the  $^{125}\text{I}$ -labeled Tyr-NCL micelles (1.8 %ID/g) after 24 h (**Fig. 7(e)**), which is probably due to the facilitation of the EPR effect (passive targeting) of the  $^{125}\text{I}$ -labeled Tyr-CL micelles based on the prolonged blood circulation time caused by the enhanced stability of the CL micelles in the blood stream.

### **3.5. Biodistribution of the boron species in the NCL and CL micelles**

To clarify the biodistribution of the boron species (VB-carborane) of the CL and NCL micelles, the concentration of boron atoms in the blood, liver, spleen, kidney and tumor samples at 24 h after intravenous injection of the NCL micelles and the CL micelles was determined using ICP-MS. As shown in **Fig. 8**, the boron concentrations in both blood (13.5 %ID/g) and tumor (5.4 %ID/g) after injection of the CL micelles were higher than those after injection of the NCL micelles (blood: 1.8 %ID/g, tumor: 1.4 %ID/g). **Fig. 9** shows the comparison of the biodistribution between  $^{125}\text{I}$ -labeled Tyr-micelles and the boron species that was determined based on radioactivity and using ICP-MS, respectively, at 24 h after injection of the CL micelles (**Fig. 9(a)**) and the NCL micelles (**Fig. 9(b)**). Almost no difference was seen in the concentration of the boron species in the CL micelles and the  $^{125}\text{I}$ -labeled Tyr-CL micelles, although low concentration of boron species was observed in the liver probably due to difficulty in complete dissolution of the large size of liver tissues with nitric acid (**Fig. 9(a)**). This finding indicates that the biodistribution of the boron species in the CL micelles was similar to that of the  $^{125}\text{I}$ -labeled Tyr-CL micelles 24 h after injection in tumor-bearing mice. In the case of the NCL micelles (**Fig. 9(b)**), however, the concentrations of the boron species in all organs and blood were lower than the concentrations of  $^{125}\text{I}$ -labeled Tyr-NCL micelles. To clarify the difference in the concentrations in blood and tumor between  $^{125}\text{I}$ -labeled Tyr-micelles and the boron species, the ratio of the concentration (%ID/g) of the CL micelles to the NCL micelles (CL/NCL) in blood and tumor, as determined based on radioactivity and using ICP-MS, were summarized in **Table 2**. The  $\text{CL}_{\text{ICP}}/\text{NCL}_{\text{ICP}}$  ratio in blood (15.8) was significantly higher than the  $\text{CL}_{\text{RI}}/\text{NCL}_{\text{RI}}$  ratio in blood (2.5). This result obviously indicates that the VB-carborane was leaked from the NCL micelles readily into the blood stream, whereas the leakage of the VB-carborane from the CL micelles might be suppressed by the existence of the cross-linking bonds between the VB-carborane and the PLA core, leading to the high accumulation of the boron species in tumor ( $\text{CL}_{\text{ICP}}/\text{NCL}_{\text{ICP}}$ : 3.8,

$CL_{RI}/NCL_{RI}$ : 1.6) through the EPR effect. Based on these results, it is concluded that the CL micelles can be used as a novel boron carrier in BNCT because the CL micelles can deliver both the polymer and the boron species into tumor tissues with high efficiency.

#### **4. Conclusion**

In conclusion, we have demonstrated the preparation of the CL micelles composed of acetal-PEG-*b*-PLA-MA and 1,2-bis(4-vinylbenzyl)-*closo*-carborane. Both the leakage of VB-carborane from the micelles and the loss of micelle integrity were suppressed even in the presence of FBS due to the introduction of cross-linking bonds between the VB-carborane and the PLA core. Additionally, the CL micelles achieved a prolonged blood circulation time and an enhanced accumulation in tumor tissues. Therefore, the CL micelles represent a promising approach to the creation of novel boron carrier for cancer BNCT, and further *in vitro* and *in vivo* BNCT studies and the improvement of the boron loading contents in the micelles are now being carried out in our laboratory.

#### **Acknowledgements**

This work was partially supported by a Grant-in-Aid for Scientific Research on Innovative Areas “Molecular Soft-Interface Science” (#20106011), from the Ministry of Education, Culture, Sports, Science and Technology of Japan (MEXT). We acknowledge Professor Takaki Kanbara, Dr. Junpei Kuwabara, and Dr. Ayako Taketoshi (University of Tsukuba) for the MS measurements.

## References

- [1] R. F. Barth, A. H. Soloway, R. G. Fairchild, R. M. Brugger, *Cancer* 70 (1992) 2995..
- [2] R. F. Barth, J. A. Coderre, M. G. H. Vincent, T. E. Blue, *Clin. Cancer Res.* 11 (2005) 3987.
- [3] C. R. Gibson, A. E. Staubus, R. F. Barth, W. Yang, N. M. Kleinholz, R. B. Jones, K. B. G-Church, W. Tjarks, A. H. Soloway, *Anal. Chem* 74. (2002) 2394.
- [4] Y. Matsumura, H. Maeda, *Cancer Res.* 46 (1984) 6387.
- [5] H. Maeda, J. Wu, T. Sawa, Y. Matsumura, K. Hori, *J. Control.Rel.* 65 (2000) 271.
- [6] G. Wu, R. F. Barth, W. Yang, R. J. Lee, W. Tjarks, M. V. Backer, J. M. Backer, *Anti-Cancer Agents in Medical Chemistry* 6 (2006) 167.
- [7] K. Maruyama, O. Ishida, S. Kasaoka, T. Takizawa, N. Utoguchi, A. Shinohara, M. Chiba, H. Kobayashi, M. Eriguchi, H. Yanagie, *J. Control. Rel.* 98 (2004) 195.
- [8] S. Masunaga, S. Kasaoka, K. Maruyama, D. Nigg, Y. Sakurai, K. Nagata, M. Suzuki, Y. Kinashi, A. Maruhashi, K. Ono, *Int. J. Radiation Oncology Biol. Phys.* 66 (2006) 1515.
- [9] D. A. Feakes, K. Shelly, M. F. Hawthorne, *Proc. Natl. Acad. Sci. U.S.A.* 92 (1995) 1367.
- [10] Y. Miyajima, H. Nakamura, Y. Kuwata, J-D. Lee, S. Masunaga, K. Ono, K. Maruyama, *Bioconjugate Chem.* 17 (2006) 1314.
- [11] J-D. Lee, M. Ueno, Y. Miyajima, H. Nakamura, *Org. Lett.* 9 (2007) 323.
- [12] T. Li, J. Hamdi, M. F. Hawthorne, *Bioconjugate Chem.* 17 (2006) 15.
- [13] K. Kataoka, A. Harada, Y. Nagasaki, *Adv. Drug Deliv. Rev.* 47 (2001) 113.
- [14] S. A. Hagan, A. G. A. Coombes, M. C. Garnett, S. E. Dunn, M. C. Davies, L. Illum, S. S. Davis, S. E. Harding, S. Purkiss, P. R. Gellert, *Langmuir* 12 (1996) 2153.
- [15] Y. Yamamoto, Y. Nagasaki, Y. Kato, Y. Sugiyama, K. Kataoka, *J. Control. Rel.* 77 (2001) 27.
- [16] S. Zhou, X. Deng, *React. & Funct. Polym.* 51 (2002) 93.

- [17] H. Chen, S. Kim, W. He, H. Wang, P. S. Low, K. Park, J. X. Cheng, *Langmuir* (2008) 5213.
- [18] A. Rösler, G. W. M. Vandermeulen, H. A. Klok, *Adv. Drug Deliv. Rev.* 53 (2001) 95.
- [19] R. K. O'Reilly, C. J. Hawker, K. L. Wooley, *Chem. Soc. Rev.* 35 (2006) 1068.
- [20] N. V. Nukolova, Z. Yang, J. O. Kim, A. V. Kabanov, T. K. Bronich, *React. & Funct. Polym.* 71 (2011) 315.
- [21] M. Iijima, Y. Nagasaki, T. Okada, M. Kato, K. Kataoka, *Macromolecules* 32 (1999) 1140.
- [22] J-H. Kim, K. Emoto, M. Iijima, Y. Nagasaki, T. Aoyagi, T. Okano, Y. Sakurai, K. Kataoka, *Polym. Adv. Technol.* 10 (1999) 647.
- [23] W. Du, Z. Xu, A. M. Nuström, K. Zhang, J. R. Leonard, K. L. Wooley, *Bioconjugate Chem.* 19 (2008) 2492.
- [24] X. Shuai, T. Merdan, A. K. Schaper, F. Xi, T. Kissel, *Bioconjugate Chem.* 15 (2004) 441.
- [25] S. R. Benhabbour, M. C. Parrott, S. E. A. Gratton, A. Adronov, *Macromolecules* 40 (2007) 5678.
- [26] R. F. Barth, D. M. Adams, A. H. Soloway, E. B. Mechetner, F. Alam, A. K. M. Anisuzzaman, *Anal. Chem.* 63 (1991) 890.
- [27] G. S. Kwon, T. Okano, *Adv. Drug Deliv. Rev.* 21 (1996) 107.
- [28] G. Gaucher, M. H. Defresne, V. P. Sant, N. Kang, D. Maysinger, J. C. Leroux, *J. Control. Rel.* 109 (2005) 169.
- [29] J. Liu, F. Zeng, C. Allen, *J. Control. Rel.* 103 (2005) 481.
- [30] Y. Yamamoto, Y. Nagasaki, M. Kato, K. Kataoka, *Colloids and Surfaces B: Biointerfaces* 16 (1999) 135.

- [31] P. Opanasopit, M. Yokoyama, M. Watanabe, K. Kawano, Y. Maitani, T. Okano, J. Control. Rel. 104 (2005) 313.
- [32] L. Wish, J. Furth, R. Srorey, Proc. Soc. Exp. Biol. Med. 74 (1950) 644.
- [33] D. E. Morrison, F. Issa, M. Bhadbhade, L. Groebler, P. K. Witting, M. Kassiou, P. J. Rutledge, L. M. Rendina, J. Biol. Inorg. Chem. 15 (2010) 1305.
- [34] F. Ahmed, D. E. Discher, J. Control. Rel. 96 (2004) 37.

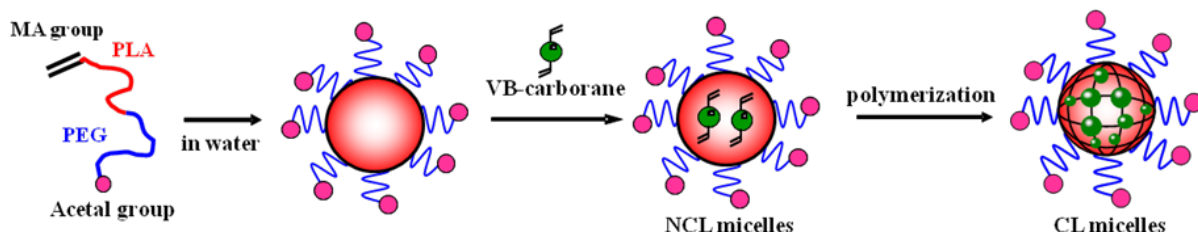


Fig. 1. Schematic illustration of the preparation of NCL and CL micelles composed of acetal-PEG-*b*-PLA-MA and polymerizable carborane (VB-carborane).

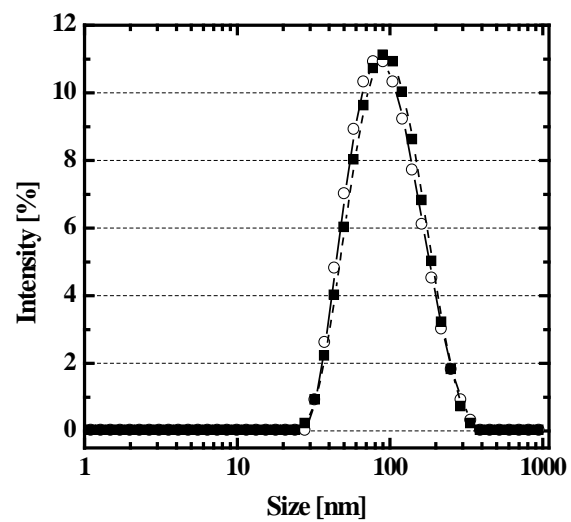


Fig. 2. Size distributions of NCL micelles (closed squares) and CL micelles (open circles).

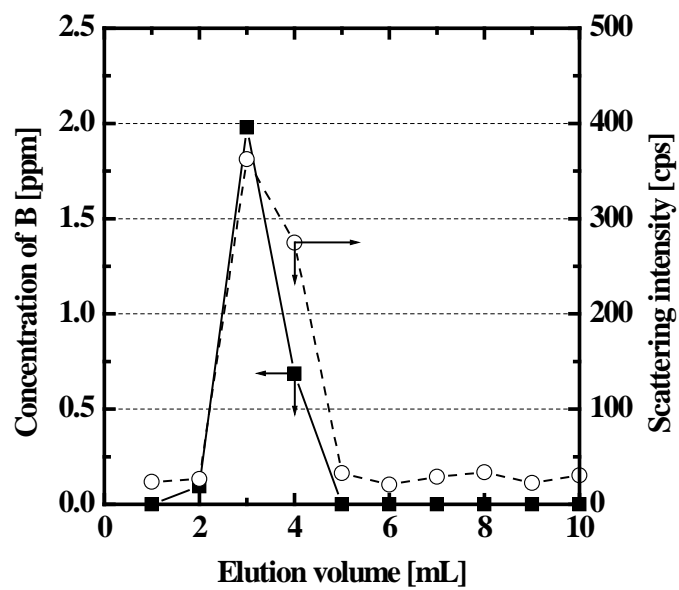


Fig. 3. Elution profiles of the CL micelles on a PD-10 (gel filtration) column. The concentration of boron atoms and the scattering intensity are indicated by the closed squares and open circles, respectively.



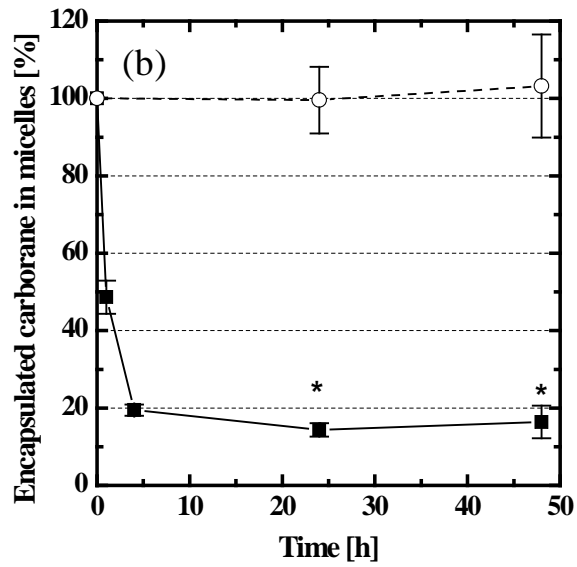
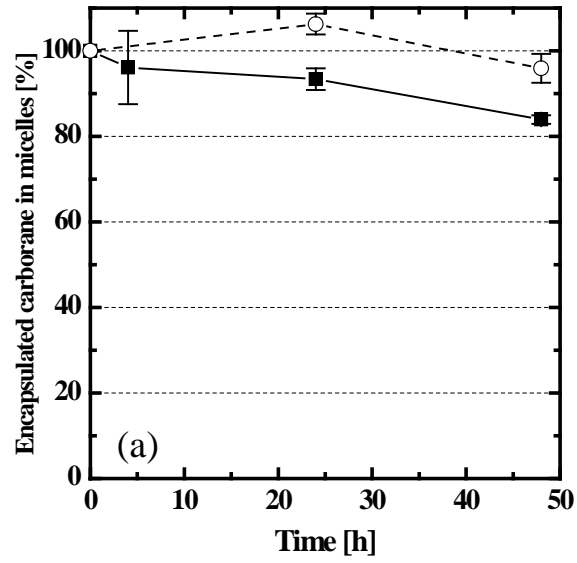


Fig. 5. Time-dependent leakage of VB-carborane from NCL micelles (closed square) and CL micelles (open circle) in the absence (a) or presence (b) of 10 % FBS at 37 °C (n = 3, mean  $\pm$  SD). \* $P < 0.01$

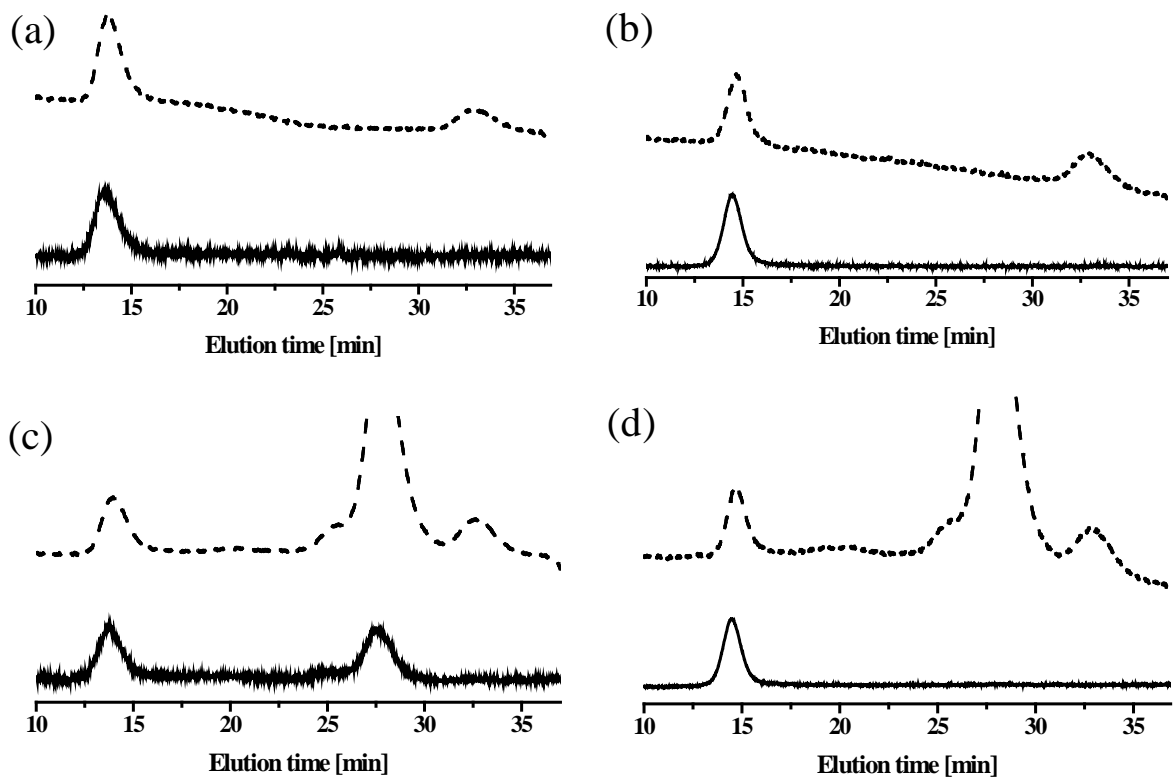


Fig. 6. SEC profiles for NCL micelles alone (a), CL micelles alone (b), NCL micelles with 10 % FBS after 24 h incubation (c), and CL micelles with 10 % FBS after incubation (d) detected with a fluorescence detection (solid line) and a refractive index detection (dashed line). (Column, Superose™ 6 10/300 GL; flow rate, 0.5 mL/min; eluent, 10 mM phosphate buffer solution, pH 7.4; temperature, 40 °C)

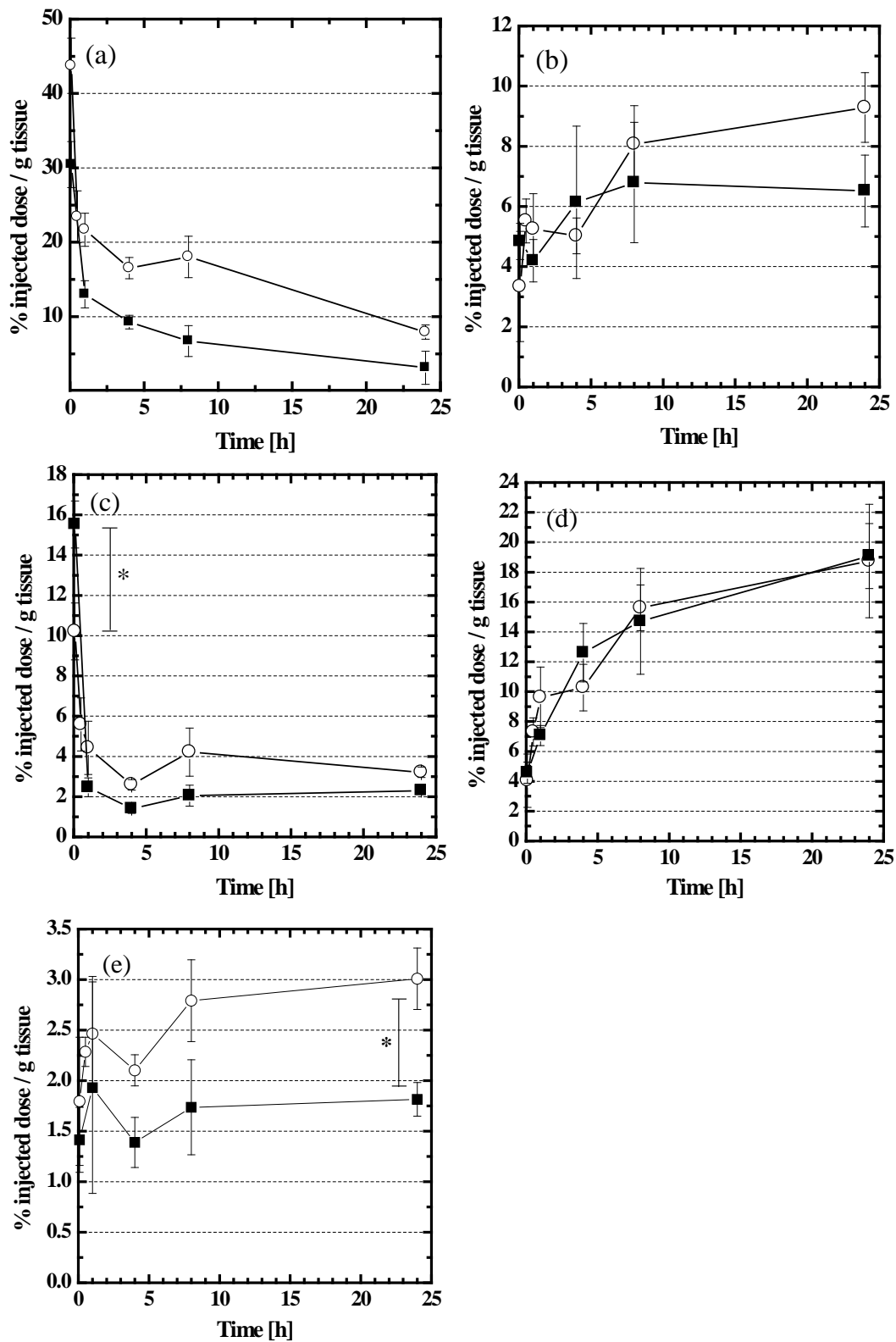


Fig. 7. Tissue distribution profiles of  $^{125}\text{I}$ -labeled Tyr-CL micelles (open circles) and  $^{125}\text{I}$ -labeled Tyr-NCL micelles (closed squares) in the blood (a), liver (b), kidney (c), spleen

(d), and tumor (e) after intravenous injection in tumor-bearing mice, determined based on radioactivity (n = 4, mean  $\pm$  SD). \* $P < 0.05$

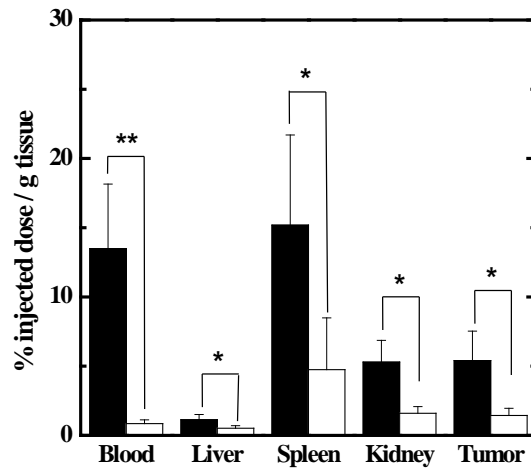


Fig. 8. Biodistribution of the boron species at 24 h after intravenous injection of CL micelles (black bars) and NCL micelles (white bars) in tumor-bearing mice, as determined by ICP-MS. (n = 4, mean  $\pm$  SD). \* $P$  < 0.05, \*\* $P$  < 0.01

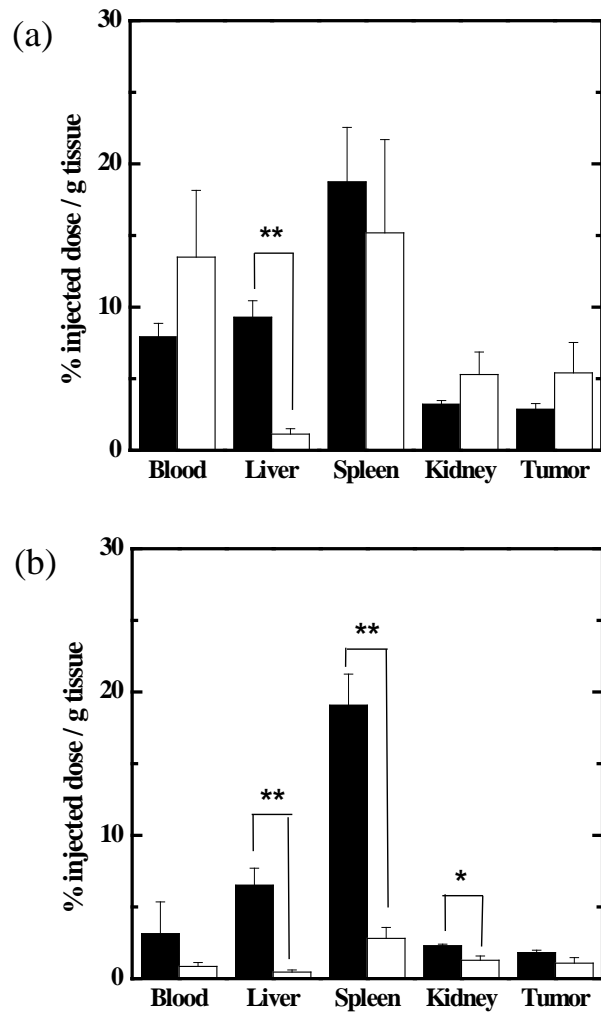


Fig. 9 The comparison of the biodistribution between  $^{125}\text{I}$ -labeled Tyr-micelles (black bars) and boron species (white bars), determined based on radioactivity and using ICP-MS, respectively, at 24 h after injection of CL micelles (a) and NCL micelles (b) in tumor-bearing mice. ( $n = 4$ , mean  $\pm$  SD). \* $P < 0.05$ , \*\* $P < 0.01$

Table 1. Characterization data of the micelles

micelles	Diameter (nm) <sup>a</sup>	Size distribution ( $\mu\text{z}/\Gamma^2$ ) <sup>a</sup>	Zeta potential (mV) <sup>b</sup>	Loading content of boron atom (wt%) <sup>c</sup>	Functionality of Tyr (mol%/polymer) <sup>d</sup>
NCL	81.1	0.158	$-0.33 \pm 0.31$	0.29	
CL	85.3	0.171	$-0.69 \pm 0.33$	0.26	
Tyr-NCL	87.1	0.192	$-0.96 \pm 0.39$	0.29	45
Tyr-CL	88.9	0.183	$-0.47 \pm 0.16$	0.27	38

<sup>a</sup> Determined by DLS at 37 °C and pH 7.4 in 10 mM phosphate buffer containing 150 mM sodium chloride.

<sup>b</sup> Determined by electrophoretic light scattering at 37 °C and pH 7.4 in 5 mM phosphate buffer (average  $\pm$  SD., n = 3).

<sup>c</sup> Determined by ICP-AES using a calibration curve based on boric acid.

<sup>d</sup> Determined by <sup>1</sup>H-NMR analysis in DMSO-*d* at 80 °C.

Table 2. The ratio of the concentration of the CL micelles to the NCL micelles (CL/NCL) in blood and tumor, as determined by radioactivity (RI) and ICP-MS (ICP).

	Blood	Tumor
RI( $CL_{RI}/NCL_{RI}$ ) <sup>a</sup>	2.5	1.6
ICP( $CL_{ICP}/NCL_{ICP}$ ) <sup>a</sup>	15.8	3.8

<sup>a</sup> Calculated by the following equation: (%ID/g of CL micelles) / (%ID/g of NCL micelles).